

Article

Phase Transformation and Hydrogen Storage Properties of an $\text{La}_{7.0}\text{Mg}_{75.5}\text{Ni}_{17.5}$ Hydrogen Storage Alloy

Lin Hu *, Rui-hua Nan *, Jian-ping Li, Ling Gao and Yu-jing Wang

School of Materials and Chemical Engineering, Xi'an Technological University, Xi'an 710021, China; jpli_0416@163.com (J.L.); Gaoling@xatu.edu.cn (L.G.); Wangyujing@xatu.edu.cn (Y.W.)

* Correspondence: hulin@xatu.edu.cn (L.H.); nanrh@xatu.edu.cn (R.N.) Tel.: +86-186-0292-5246 (L.H.)

Academic Editor: Peter Lagerlof

Received: 25 September 2017; Accepted: 16 October 2017; Published: 18 October 2017

Abstract: X-ray diffraction showed that an $\text{La}_{7.0}\text{Mg}_{75.5}\text{Ni}_{17.5}$ alloy prepared via inductive melting was composed of an $\text{La}_2\text{Mg}_{17}$ phase, an LaMg_2Ni phase, and an Mg_2Ni phase. After the first hydrogen absorption/desorption process, the phases of the alloy turned into an La–H phase, an Mg phase, and an Mg_2Ni phase. The enthalpy and entropy derived from the van't Hoff equation for hydriding were $-42.30 \text{ kJ}\cdot\text{mol}^{-1}$ and $-69.76 \text{ J}\cdot\text{K}^{-1}\cdot\text{mol}^{-1}$, respectively. The hydride formed in the absorption step was less stable than MgH_2 ($-74.50 \text{ kJ}\cdot\text{mol}^{-1}$ and $-132.3 \text{ J}\cdot\text{K}^{-1}\cdot\text{mol}^{-1}$) and Mg_2NiH_4 ($-64.50 \text{ kJ}\cdot\text{mol}^{-1}$ and $-123.1 \text{ J}\cdot\text{K}^{-1}\cdot\text{mol}^{-1}$). Differential thermal analysis showed that the initial hydrogen desorption temperature of its hydride was 531 K. Compared to Mg and Mg_2Ni , $\text{La}_{7.0}\text{Mg}_{75.5}\text{Ni}_{17.5}$ is a promising hydrogen storage material that demonstrates fast adsorption/desorption kinetics as a result of the formation of an La–H compound and the synergetic effect of multiphase.

Keywords: hydrogen storage alloy; phase transition; La hydride compound; hydriding kinetic

1. Introduction

Hydrogen is considered a promising energy carrier to replace the traditional fossil fuels because it is abundant, lightweight, and environmentally friendly, and has high energy content ($142 \text{ MJ}\cdot\text{kg}^{-1}$) [1]. As an ideal energy carrier, hydrogen can be easily converted into a needed form of energy without releasing harmful emissions [2]. However, up to now, highly efficient hydrogen storage technology remains challenging, as the practical application of hydrogen energy is constrained [3]. More attention has been paid to magnesium hydride (MgH_2), which is a highly promising material for hydrogen storage given its high hydrogen storage capacity (7.6 wt %), low density, good reversibility, and low cost [4–8]. Unfortunately, its practical application in hydrogen storage is limited by slow absorption/desorption kinetics and high thermodynamic stability ($\Delta H = -74.50 \text{ kJ}\cdot\text{mol}^{-1} \text{ H}_2$) [9,10]. In the past several decades, Mg has been alloyed with various metals to form Mg-based alloys to improve its hydrogenation properties. In numerous Mg-based alloys, rare-earth (RE) Mg alloys and Mg-transition metal alloys have been intensively investigated. An La–Mg alloy was first reported by Hagenmull et al. in 1980 with admirable hydrogen storage properties [11], and Zou et al. [12] found that RE (RE = Nd, Gd, Er) in solid state solutions in Mg contribute to the improved hydrogenation thermodynamics and kinetics of Mg ultrafine particles. Considering the relatively fine hydrogen storage properties, Mg_2Ni alloys are a classic material in Mg-transition metal alloys [13].

In recent studies, ternary alloys defined as La–Mg–Ni alloys was successfully developed by introducing Ni into $\text{La}_2\text{Mg}_{17}$. This material with the optimized composition of LaMg_2Ni exhibited a relatively low hydrogen desorption temperature and fine kinetic properties [14]. However, the

hydrogen storage capacity of this alloy was dramatically reduced by excessive un-hydrogenation elements such as La and Ni. A feasible method of improving the hydrogenation capacity of an La–Mg–Ni alloy is to increase the account of Mg in the alloy. Balcerzak investigated the hydrogen storage capacity of $\text{La}_{2-x}\text{Mg}_x\text{Ni}_7$ alloys ($x = 0, 0.25, 0.5, 0.75, 1$). It was observed that the gaseous hydrogen storage capacity of La–Mg–Ni alloys increases with Mg content to a maximum in $\text{La}_{1.5}\text{Mg}_{0.5}\text{Ni}_7$ alloys [15]. In this paper, an $\text{La}_{7.0}\text{Mg}_{75.5}\text{Ni}_{17.5}$ alloy was prepared by inductive melting to achieve a uniform phase distribution. Their hydrogenation properties and phase transformation in the hydrogen storage cycles were further investigated to evaluate their potential for application in hydrogen storage.

2. Experimental Section

An $\text{La}_{7.0}\text{Mg}_{75.5}\text{Ni}_{17.5}$ alloy ingot was prepared by inductive melting of high-purity La, Mg, and Ni (purity more than 99.9%) in a magnesia crucible under an argon atmosphere. The ingots were mechanically crushed and ground in air into fine powders. Powders with particle sizes of 38–74 μm were used in a P–C–T test, and those with particle sizes less than 38 μm were used in X-ray diffraction analysis. The phase structure of the as-cast alloy and the hydrogenated alloy were measured with a D/max-2500/PC X-ray diffractometer (Rigaku, Tokyo, Japan) with Cu $K\alpha$ radiation and analyzed using Jade-5.0 software. Scanning electron microscopy (SEM) images of the $\text{La}_{7.0}\text{Mg}_{75.5}\text{Ni}_{17.5}$ alloy were obtained with a HITACHI S-4800 scanning electron microscope (Hitachi, Tokyo, Japan) with an energy dispersive X-ray spectrometer (EDS) (Shimadzu, Kyoto, Japan). Hydrogen storage property measurements were carried out using P–C–T characteristic measurement equipment (Suzuki Shokan, Tokyo, Japan). The measurement conditions were as follows: delay time: 300 s; maximum pressure: 3 MPa. The hydriding kinetic of the as-cast alloy was also tested via P–C–T characteristic measurement equipment under a hydrogen pressure of 3 MPa.

3. Results and Discussion

No standard powder diffraction pattern for LaMg_2Ni is available in any of the ICDD (International Center for Diffraction Data) files. For a clear, standard XRD pattern of LaMg_2Ni , the cell parameters and atom positions for single crystal alloys are listed in Table 1. Its crystal structure was drawn with Diamond 3.0 software in Figure 1. It can be seen that the $\text{La}_{7.0}\text{Mg}_{75.5}\text{Ni}_{17.5}$ alloy had a multiphase structure containing an LaMg_2Ni phase with a CuMgAl_2 -type structure [16–18], an $\text{La}_2\text{Mg}_{17}$ phase with an $\text{Ni}_{17}\text{Th}_2$ -type structure, and an Mg_2Ni phase. No La–Ni phase was observed, which is ascribed to the abundant Mg atoms in the alloy; thus, the La and Ni atoms are a solid solute and readily alloy with the Mg.

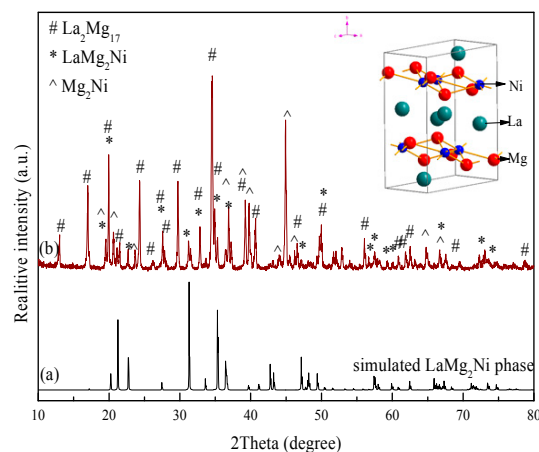


Figure 1. XRD patterns of the $\text{La}_{7.0}\text{Mg}_{75.5}\text{Ni}_{17.5}$ alloy: (a) simulated LaMg_2Ni phase; (b) as-cast and crystal structure of LaMg_2Ni .

Table 1. X-ray structure refinement results on a single crystal of LaMg₂Ni.

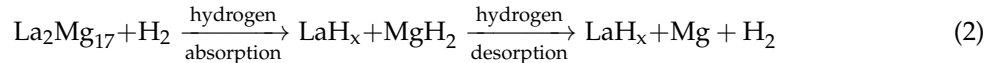
Phase	Cell Parameters (Å)			Atom Position					References
	<i>a</i>	<i>b</i>	<i>c</i>	Atoms	<i>x</i>	<i>y</i>	<i>z</i>	Site	
LaMg ₂ Ni	4.2266	10.3031	8.3601	La	0	0.4402	1/4	4c	[10]
				Mg	0	0.1543	0.0552	8f	
				Ni	0	0.7266	1/4	4c	

Figure 2 shows the SEM micrographs of the La_{7.0}Mg_{75.5}Ni_{17.5} alloy, and its EDS analysis is listed in Table 2. The La_{7.0}Mg_{75.5}Ni_{17.5} alloy contains three distinct crystallography phases: the first is the La₂Mg₁₇ phase in the black region (identified as A), the second is the LaMg₂Ni phase in the bright region (identified as B), and the third is the Mg₂Ni phase in the dark region (identified as C). According to the EDS analysis results of the phases in the alloy, which are listed in Table 2, the determinations of the phases correspond to the XRD analyses.

The phase constituent of the alloys after dehydrogenation is presented in Figure 3. The peaks of LaH_{2.46}, Mg, Mg₂Ni, and MgH₂ were observed after the hydrogen desorption process. When hydrogenation is carried out, the LaMg₂Ni phase decomposes to an La phase and an Mg₂Ni phase, the La phase then forms a stable La hydride, and the Mg₂Ni turns into Mg₂NiH₄ in the hydrogen atmosphere [19,20]. The reaction of the LaMg₂Ni phase can be summarized as follows:



The La₂Mg₁₇ phase decomposed to an La phase and an Mg phase. Then, the La phase turned into La-H, and Mg changed into MgH₂. The phase transformation of La₂Mg₁₇ can be described as



The Mg₂Ni phase turns into Mg₂NiH₄ when it absorbs hydrogen, and turns back into Mg₂Ni in the hydrogen desorption process. The MgH₂ phase can be seen in Figure 3, which shows that the hydrogen desorption process of the alloy is incomplete.

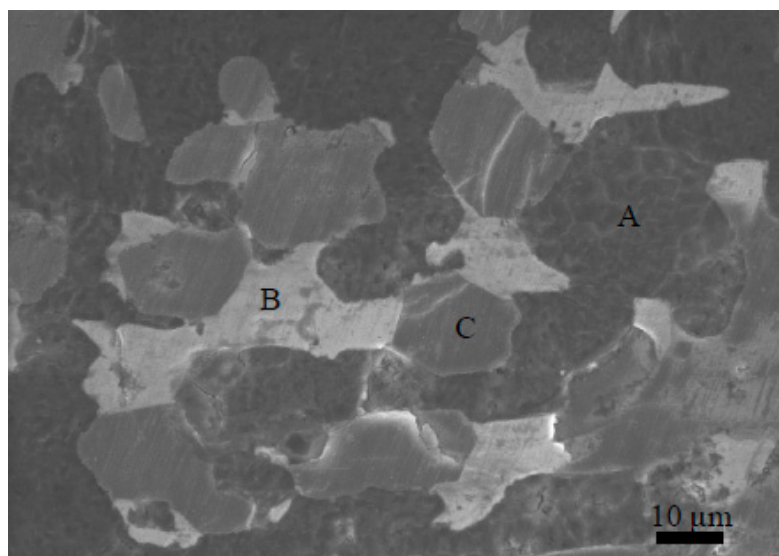
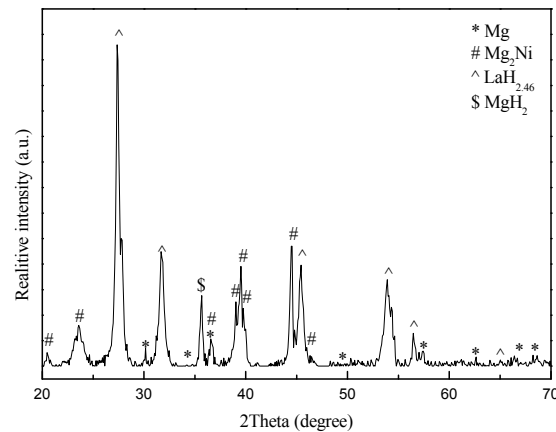


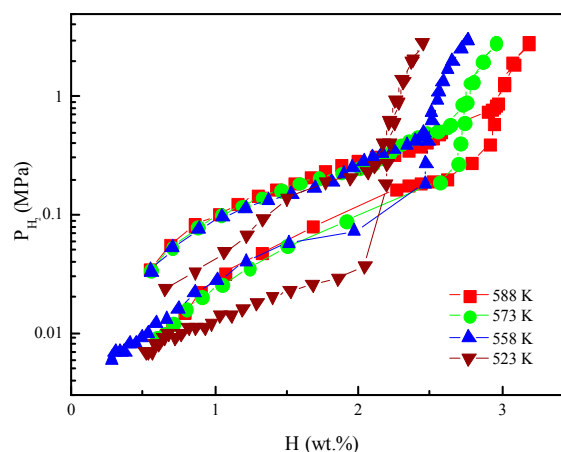
Figure 2. SEM micrographs and elements distribution images on the surface of the La_{7.0}Mg_{75.5}Cu_{17.5} alloy.

Table 2. EDS analysis of the $\text{La}_{7.0}\text{Mg}_{75.5}\text{Ni}_{17.5}$ alloy.

Elements (at.%)	La	Mg	Ni
A	11.01	88.04	0.95
B	26.08	49.04	24.88
C	0.89	65.05	34.06

**Figure 3.** XRD pattern of the dehydrogenated $\text{La}_{7.0}\text{Mg}_{75.5}\text{Ni}_{17.5}$ alloy.

The P–C–T curves of the $\text{La}_{7.0}\text{Mg}_{75.5}\text{Ni}_{17.5}$ alloy at different temperatures are shown in Figure 4. Because of the decomposition of the LaMg_2Ni phase and the $\text{La}_2\text{Mg}_{17}$ phase, the actual absorb/desorb hydrogen phase are the Mg phase and the Mg_2Ni phase, which is consistent with the XRD pattern of the dehydrogenated alloy in Figure 3. A slant plateau can be observed in each hydrogen absorb/desorb process, indicating that the amount of H solute in the alloy increases with the rise of H pressure. This is due to the multiphase structure of the alloy, which is abundant in phase interfaces. H atoms readily enter the interfaces and then compose with Mg or Mg_2Ni to form the MgH_2 and Mg_2NiH_4 . With the reduction of hydrogenation temperature, the maximum capacity of the $\text{La}_{7.0}\text{Mg}_{75.5}\text{Ni}_{17.5}$ alloy decreased from 3.18 wt % (588 K) to 2.45 wt % (523 K), suggesting that the activity of the interface is restricted by a relatively low temperature.

**Figure 4.** The P–C–T curves of the $\text{La}_{7.0}\text{Mg}_{75.5}\text{Ni}_{17.5}$ alloy at different temperatures.

In order to obtain the thermodynamic parameters of the hydriding reaction of the $\text{La}_{7.0}\text{Mg}_{75.5}\text{Ni}_{17.5}$ alloy, the plateau pressure (P , absolute atmosphere) and temperature (T , in K) are plotted according to the van't Hoff equation (Equation (3)).

$$\ln K = \frac{\Delta H}{RT} - \frac{\Delta S}{R} \quad (3)$$

where K is the equilibrium constant ($K = 1/P_{H_2}$ in the hydriding process) and the van't Hoff plots are demonstrated in Figure 5. According to the van't Hoff equation, the enthalpy and entropy for the hydriding reaction are calculated to be $-42.30 \text{ kJ}\cdot\text{mol}^{-1}$ and $-69.76 \text{ J}\cdot\text{K}^{-1}\cdot\text{mol}^{-1}$, respectively. The results show that the alloy has a low enthalpy, its absolute value is lower than those of MgH_2 and Mg_2NiH_4 . The improvement on the hydrogen storage properties of the $\text{La}_{7.0}\text{Mg}_{75.5}\text{Ni}_{17.5}$ alloy is because of the existence of LaH , which can reduce the enthalpy change of the hydriding process of the Mg and Mg_2Ni phase in this alloy. The main reason for these experimental results is that LaH can increase the reactive surface area and dramatically reduce the diffusion length of hydrogen.

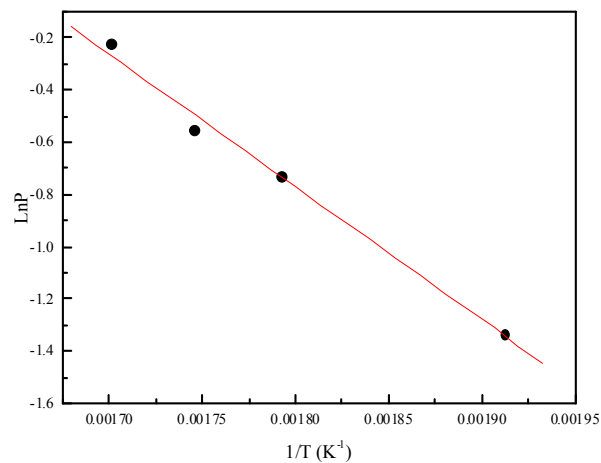


Figure 5. The van't Hoff plot of the alloy in hydrogenation processes.

The hydriding/dehydriding processes kinetic curves of the $\text{La}_{7.0}\text{Mg}_{75.5}\text{Ni}_{17.5}$ alloy at different temperatures are shown in Figure 6. Figure 6a shows that the uptake time for the hydrogen content to reach 90% of the maximum storage capacity was less than 60 s at various temperatures. The amount of hydrogen desorption increased as the temperature increased. Figure 7 compares the dehydriding kinetic curves of $\text{La}_{7.0}\text{Mg}_{75.5}\text{Ni}_{17.5}$ with that of pure MgH_2 powder at 573 K. The hydride of the alloy presented a significant improvement on both hydrogen desorption kinetics and hydrogen absorption capacities. During 1800 s, 0.99 wt % hydrogen desorbed from the hydride of the $\text{La}_{7.0}\text{Mg}_{75.5}\text{Ni}_{17.5}$ alloy, while pure MgH_2 powder only desorbed 0.39 wt % hydrogen.

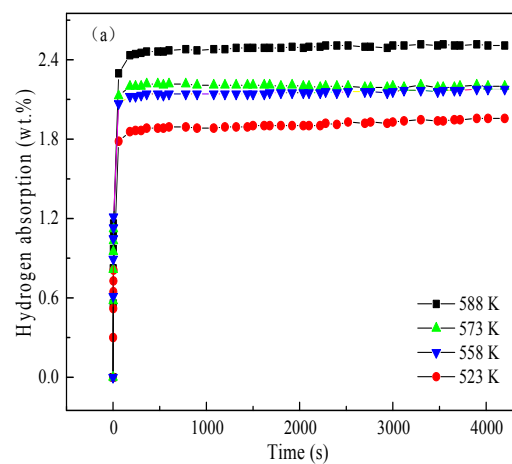


Figure 6. Cont.

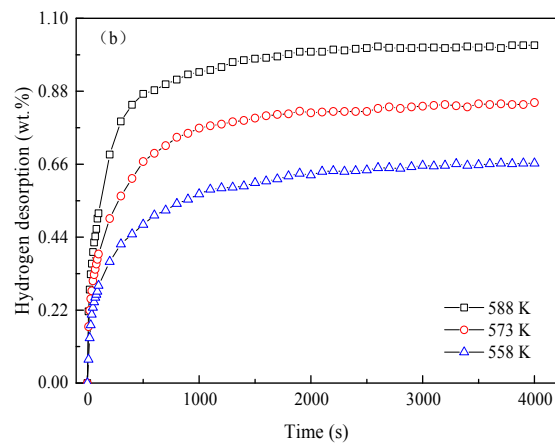


Figure 6. Kinetics of the $\text{La}_{7.0}\text{Mg}_{75.5}\text{Ni}_{17.5}$ alloy at different temperatures: (a) hydriding processes, (b) dehydriding processes.

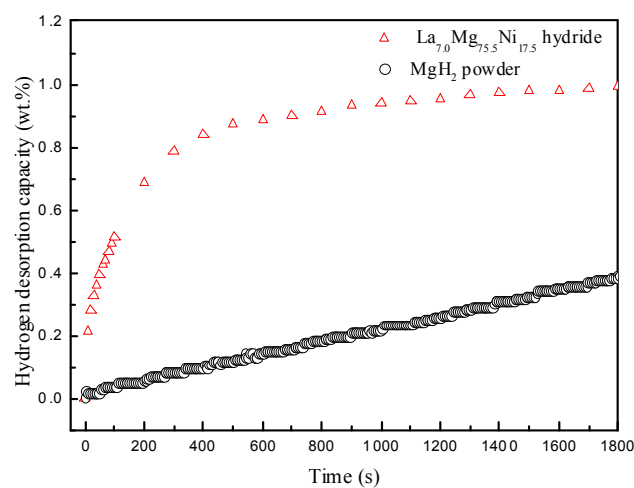


Figure 7. Dehydriding kinetics of the $\text{La}_{7.0}\text{Mg}_{75.5}\text{Ni}_{17.5}$ alloy and MgH_2 at 573 K.

The differential thermal analysis (DTA) of MgH_2 , Mg_2NiH_4 , and hydride of the $\text{La}_{7.0}\text{Mg}_{75.5}\text{Ni}_{17.5}$ alloy are presented in Figure 8. It can be seen that the initial hydrogen desorption temperature of the alloy hydride of 531 K was lower than that of MgH_2 (714 K) and Mg_2NiH_4 (549 K). The ameliorations on the thermo and kinetic properties of $\text{La}_{7.0}\text{Mg}_{75.5}\text{Ni}_{17.5}$ are attributed to the facts that hydrogen atoms in its hydride increase the crystalline parameters and further enhance the interaction between the MgH_2 phase and the Mg_2NiH_4 phase. This interaction evolves into a synergetic effect in the multiphase structure and facilitates its hydrogen desorption [21,22]. During dehydrogenation, Mg_2NiH_4 first desorbed hydrogen and exhibited a significant volume contraction, causing a significant contraction strain of MgH_2 . Therefore, it increased the energy of the MgH_2 phase and advantaged the dehydrogenation of the MgH_2 phase [23–25].

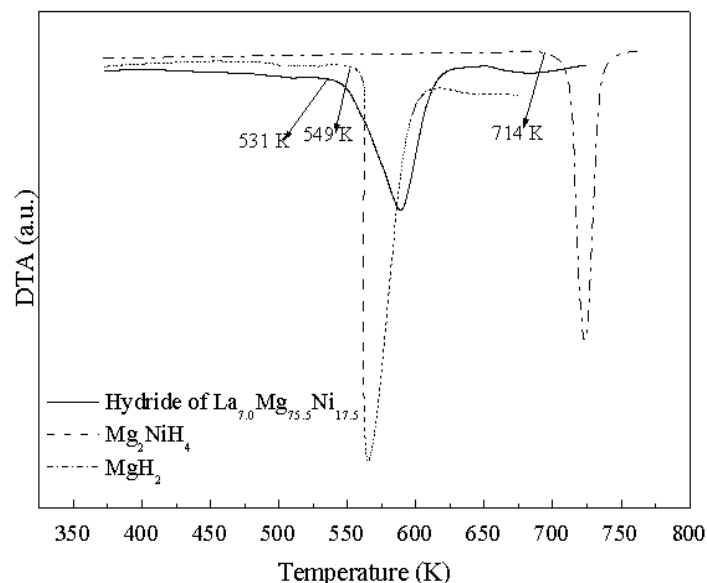


Figure 8. DTA curves of MgH_2 , Mg_2NiH_4 , and hydride of the $\text{La}_{7.0}\text{Mg}_{75.5}\text{Ni}_{17.5}$ alloy.

4. Conclusions

The phase transformation and hydrogen storage properties of a multiphase $\text{La}_{7.0}\text{Mg}_{17.5}\text{Ni}_{17.5}$ alloy were investigated in this work. The hydriding process leads to the formation of the La–H, Mg_2NiH_4 , and MgH_2 phases. The hydrogen absorption capacity is 2.45 wt % at 523 K. A low enthalpy ($-42.30 \text{ kJ}\cdot\text{mol}^{-1}$) that is lower than that of MgH_2 ($-74.50 \text{ kJ}\cdot\text{mol}^{-1}$) and Mg_2NiH_4 ($-74.50 \text{ kJ}\cdot\text{mol}^{-1}$) was obtained. The uptake time for hydrogen content to reach 90% of the maximum storage capacity for the $\text{La}_{7.0}\text{Mg}_{75.5}\text{Ni}_{17.5}$ alloy was less than 60 s at all testing temperatures, and the initial hydrogen desorption temperature of the alloy hydride (531 K) was lower than both MgH_2 (714 K) and Mg_2NiH_4 (549 K). Generally, the dissociation of magnesium hydride does not occur below 573 K. Improvement in the hydrogen storage properties of the $\text{La}_{7.0}\text{Mg}_{75.5}\text{Ni}_{17.5}$ alloy is due to the presence of La–H and the synergistic effect between the phases during the hydriding/dehydriding process.

Acknowledgments: This research was supported by the National Natural Science Foundation of China (51502235 and 51502234), the President's Fund of Xi'an Technological University (XAGDXJJ5011), and the Natural Science Basic Research Plan in Shaanxi Province of China (2016JQ5011).

Author Contributions: Hu Lin designed the research and wrote the manuscript. Nan Ruihua, Gao Ling, and Wang Yujing performed experiments, collected data, and generated the figures. Both authors contributed to editing and reviewing the manuscript.

Conflicts of Interest: The authors declare no conflict of interest.

References

1. Liu, T.; Shen, H.L.; Liu, Y.; Xie, L. Scaled-up synthesis of nanostructured Mg-based compounds and their hydrogen storage properties. *J. Power Sources* **2013**, *227*, 86–93. [[CrossRef](#)]
2. Liu, Y.F.; Yang, Y.X.; Gao, M.X.; Pan, H.G. Tailoring Thermodynamics and Kinetics for Hydrogen Storage in Complex Hydrides towards Applications. *Chem. Rec.* **2016**, *16*, 189–204. [[CrossRef](#)]
3. Ma, X.J.; Xie, X.B.; Liu, P.; Xu, L.; Liu, T. Synergistic catalytic effect of Ti hydride and Nb nanoparticles for improving hydrogenation and dehydrogenation kinetics of Mg-based nanocomposite. *Prog. Nat. Sci-Mater.* **2017**, *27*, 99–104. [[CrossRef](#)]
4. Zhu, X.L.; Pei, L.C.; Zhao, Z.Y. The catalysis mechanism of La hydrides on hydrogen storage properties of MgH_2 in $\text{MgH}_2 + x \text{ wt.}\% \text{ LaH}_3$ ($x = 0, 10, 20, \text{ and } 30$) composites. *J. Alloys Compd.* **2013**, *557*, 64–69. [[CrossRef](#)]
5. Hu, L.; Han, M.; Li, J.H. Phase structure and hydrogen absorption property of LaMg_2Cu . *Mater. Sci. Eng. B.* **2010**, *166*, 209–212. [[CrossRef](#)]

6. Hu, L.; Han, S.M.; Yang, C. Phase Structure and Hydrogen Storage Property of $\text{LaMg}_2\text{Cu}_{1-x}\text{Ni}_x$ ($x = 0\text{--}0.90$) Alloys. *Chin. J. Inorg. Chem.* **2010**, *26*, 1044–1048. [[CrossRef](#)]
7. Abdellatif, M.; Campostrini, R.; Leoni, M. Effects of SnO_2 on hydrogen desorption of MgH_2 . *Int. J. Hydrog. Energy* **2013**, *38*, 4664–4669. [[CrossRef](#)]
8. Pei, P.; Song, X.P.; Liu, J. Study on the hydrogen desorption mechanism of a Mg-V composite prepared by SPS. *Int. J. Hydrog. Energy* **2012**, *37*, 984–989. [[CrossRef](#)]
9. Ares, J.R.; Leardini, F.; Díaz-Chao, P. Hydrogen desorption in nanocrystalline MgH_2 thin films at room temperature. *J. Alloys Compd.* **2010**, *495*, 650–654. [[CrossRef](#)]
10. Wang, H.; Zhang, J.; Liu, J.W. Improving hydrogen storage properties of MgH_2 by addition of alkali hydroxides. *Int. J. Hydrog. Energy* **2013**, *38*, 10932–10938. [[CrossRef](#)]
11. Darriet, B.; Pezat, M.; Hbika, A. Application of magnesium rich rare-earth alloys to hydrogen storage. *Int. J. Hydrog. Energy* **1980**, *5*, 173–178. [[CrossRef](#)]
12. Zou, J.X.; Zeng, X.Q.; Ying, Y.J. Study on the hydrogen storage properties of core-shell structured Mg-RE (RE = Nd, Gd, Er) nano-composites synthesized through arc plasma method. *Int. J. Hydrog. Energy* **2013**, *19*, 2337–2346. [[CrossRef](#)]
13. Atias-Adrian, I.C.; Deorsola, F.A.; Ortigoza-Villalba, G.A. Development of nanostructured Mg_2Ni alloys for hydrogen storage applications. *Int. J. Hydrog. Energy* **2011**, *36*, 7897–7910. [[CrossRef](#)]
14. Li, X.; Yang, T.; Zhang, Y.H. Kinetic properties of $\text{La}_2\text{Mg}_{17-x}$ wt.% Ni ($x = 0\text{--}200$) hydrogen storage alloys prepared by ball milling. *Int. J. Hydrog. Energy* **2014**, *39*, 13557–13563. [[CrossRef](#)]
15. Balcerzak, M.; Nowak, M.; Jurczyk, M. Hydrogenation and electrochemical studies of La-Mg-Ni alloys. *Int. J. Hydrog. Energy* **2017**, *42*, 1436–1443. [[CrossRef](#)]
16. Lin, H.J.; Ouyang, L.Z.; Wang, H. Phase transition and hydrogen storage properties of melt-spun $\text{Mg}_3\text{LaNi}_{0.1}$ alloy. *Int. J. Hydrog. Energy* **2012**, *37*, 1145–1150. [[CrossRef](#)]
17. Renaudin, G.; Guenee, L.; Yvon, K. $\text{LaMg}_2\text{NiH}_7$, a novel quaternary metal hydride containing tetrahedral $[\text{NiH}_4]^{4-}$ complexes and hydride anions. *J. Alloys Compd.* **2003**, *350*, 145–150. [[CrossRef](#)]
18. Rodewald, U.C.; Chevalier, B.; Pöttgen, R. Rare earth-transition metal-magnesium compounds—An overview. *J Solid State Chem.* **2007**, *180*, 1720–1736. [[CrossRef](#)]
19. Negri, S.D.; Giovannini, M.; Saccone, A. Constitutional properties of the La-Cu-Mg system at 400 °C. *J. Alloys Compd.* **2006**, *427*, 134–141. [[CrossRef](#)]
20. Chio, M.D.; Ziggotti, A.; Baricco, M. Effect of microstructure on hydrogen absorption in LaMg_2Ni . *Intermetallics* **2008**, *16*, 102–106. [[CrossRef](#)]
21. Teresiak, A.; Uhlemann, M.; Thomas, J. Influence of Co and Pd on the formation of nanostructured LaMg_2Ni and its hydrogen reactivity. *J. Alloys Compd.* **2014**, *582*, 647–658. [[CrossRef](#)]
22. Pei, L.C.; Han, S.M.; Zhu, X.L. Effect of La hydride Compound on Hydriding Process of Mg_2Ni Phase in LaMg_2Ni Alloy. *Chin. J. Inorg. Chem.* **2012**, *28*, 1489–1494.
23. Zaluska, A.; Zaluski, L.; Ström-Olsen, J.O. Synergy of hydrogen sorption in ball-milled hydrides of Mg and Mg_2Ni . *J. Alloys Compd.* **1999**, *289*, 197–206. [[CrossRef](#)]
24. Li, Z.N.; Jiang, L.J.; Liu, X.P. Dehydriding properties of Mg-20%(RE-Ni)(RE = La, Y, Mm) composites. *J. Chin. Rare Earth Soc.* **2008**, *26*, 624–628.
25. Zhang, H.G.; Lv, P.; Wang, Z.M. Effect of Mg content on structure, hydrogen storage properties and thermal stability of melt-spun $\text{Mg}_x(\text{LaNi}_3)_{100-x}$ alloys. *Int. J. Hydrog. Energy* **2014**, *39*, 9267–9275. [[CrossRef](#)]

